Published in final edited form as:
Nature. 2008 July 10; 454(7201): 232–235. doi:10.1038/nature07006.

Essential role for Nix in autophagic maturation of erythroid cells

Hector Sandoval[1], **Perumal Thiagarajan**[2], **Swapan K. Dasgupta**[2], **Armin Schumacher**[3], **Josef T. Prchal**[4], **Min Chen**[1], and **Jin Wang**[1]

1*Department of Immunology, Baylor College of Medicine, Houston, Texas 77030, USA.*

2*Department of Pathology, Baylor College of Medicine, Houston, Texas 77030, USA.*

3*Department of Molecular and Human Genetics, Baylor College of Medicine, Houston, Texas 77030, USA.*

4*Division of Hematology, University of Utah, School of Medicine, Salt Lake City, Utah 84132, USA.*

Abstract

Erythroid cells undergo enucleation and the removal of organelles during terminal differentiation[1–3]. Although autophagy has been suggested to mediate the elimination of organelles for erythroid maturation[2–6], the molecular mechanisms underlying this process remain undefined. Here we report a role for a Bcl-2 family member, *Nix* (also called Bnip3L)[7–9], in the regulation of erythroid maturation through mitochondrial autophagy. $Nix^{-/-}$ mice developed anaemia with reduced mature erythrocytes and compensatory expansion of erythroid precursors. Erythrocytes in the peripheral blood of $Nix^{-/-}$ mice exhibited mitochondrial retention and reduced lifespan *in vivo*. Although the clearance of ribosomes proceeded normally in the absence of Nix, the entry of mitochondria into autophagosomes for clearance was defective. Deficiency in Nix inhibited the loss of mitochondrial membrane potential ($\Delta\Psi_m$), and treatment with uncoupling chemicals or a BH3 mimetic induced the loss of $\Delta\Psi_m$ and restored the sequestration of mitochondria into autophagosomes in $Nix^{-/-}$ erythroid cells. These results suggest that Nix-dependent loss of $\Delta\Psi_m$ is important for targeting the mitochondria into autophagosomes for clearance during erythroid maturation, and interference with this function impairs erythroid maturation and results in anaemia. Our study may also provide insights into molecular mechanisms underlying mitochondrial quality control involving mitochondrial autophagy.

Nix, a BH3-only member of the Bcl-2 family, is upregulated in erythroid cells undergoing terminal differentiation[10]. To determine the potential function for Nix in erythroid maturation, we generated $Nix^{-/-}$ mice using embryonic stem (ES) cells with a gene trap insertion between exons 3 and 4 of *Nix* (Supplementary Fig. 2). We first examined red blood cells in the peripheral blood (RBCs), including reticulocytes and erythrocytes, in $Nix^{-/-}$ mice. Although RBC counts were decreased (Supplementary Table 1), polychromasia and increased reticulocytes were observed in $Nix^{-/-}$ mice (Fig. 1a and Supplementary Fig. 3a). We also examined RBCs for the expression of an erythroid cell marker, glycophorin-A-associated Ter119, and for transferrin receptor CD71, which is downregulated during terminal erythroid differentiation [11,12]. Although $Ter119^{low}CD71^{high}$ and $Ter119^{+}$ $CD71^{high}$ early erythroblasts[13] were absent in the peripheral blood, a significant increase in $Ter119^{+}$ $CD71^{+}$ reticulocytes was observed in $Nix^{-/-}$ mice (Fig. 1b). Electron microscopy also showed more irregularly shaped cells

Correspondence and requests for materials should be addressed to M.C. (minc@bcm.tmc.edu) or J.W. (jinwang@bcm.tmc.edu).
Author Contributions H.S. conducted the majority of the experiments, supervised by J.W. and M.C.; P.T. stained spleen sections and blood smears; S.K.D. measured osmotic fragility and assisted with biotin and CMFDA labelling; A.S. performed RT–PCR for *Epo*; J.T.P. and P.T. provided experimental advice; M.C. and J.W. generated the $Nix^{-/-}$ mice, designed experiments and prepared the manuscript; and all authors edited the manuscript.
Author Information Reprints and permissions information is available at http://www.nature.com/reprints.

characteristic of reticulocytes in the peripheral blood of *Nix*$^{-/-}$ mice (Supplementary Fig. 3c). In contrast, CD71^{-} mature erythrocytes were reduced in *Nix*$^{-/-}$ mice (Fig. 1b). Together, these data suggest a potential defect in the development from CD71^{+} reticulocytes into mature CD71^{-} erythrocytes in *Nix*$^{-/-}$ mice.

Terminal differentiation of reticulocytes into erythrocytes involves the coordinated removal of organelles[14]. Because Nix localizes to the mitochondria[10], we examined whether *Nix*$^{-/-}$ reticulocytes might be defective in eliminating the mitochondria. Consistent with increased reticulocytes, more RBCs (28% at 3 weeks and 12% at 6 weeks of age) were positive for CD71 and mitochondrial staining in *Nix*$^{-/-}$ mice than in wild-type controls (Fig. 1c). Notably, a significant portion of CD71^{-} RBCs in *Nix*$^{-/-}$ mice retained mitochondria (33% and 24% of total RBCs in 3-week-old and 6-week-old mice, respectively), whereas mitochondria were virtually absent in wild-type CD71^{-} RBCs (Fig. 1c). Immunocytochemistry staining for COX IV, a catalytic subunit of cytochrome *c* oxidase localized to the inner mitochondrial membrane, also confirmed the presence of mitochondria in both CD71^{+} and CD71^{-} RBCs in *Nix*$^{-/-}$ mice (Fig. 1d). Electron microscopy revealed that very few RBCs in wild-type mice contained mitochondria or detectable autophagosomes (Fig. 1e). Autophagosomal structures were abundant in *Nix*$^{-/-}$ RBCs (Fig. 1e). However, all *Nix*$^{-/-}$ RBCs containing autophagosomes also displayed multiple mitochondria outside of autophagosomes, while approximately 20% of autophagosomes contained one mitochondrion inside (Fig. 1e). This suggests a potential defect in the inclusion of mitochondria by autophagosomes for clearance in *Nix*$^{-/-}$ RBCs.

The loading and unloading of oxygen by haemoglobin can induce oxidant stress in RBCs[15]. The mitochondrion is a major site for the production of reactive oxygen species (ROS) and can function as an apoptotic machinery[16]. The removal of mitochondria is therefore potentially beneficial for the survival of RBCs. We therefore examined whether Nix deficiency could affect RBC survival *in vivo*. Wild-type and *Nix*$^{-/-}$ mice were injected with *N*-hydroxysuccinimido (NHS)-biotin. Cell clearance was determined by the loss of biotinylated RBCs[17]. We observed that biotinylated RBCs disappeared more rapidly in *Nix*$^{-/-}$ mice than in wild-type controls (Fig. 2a, top panel), suggesting a faster clearance of RBCs in *Nix*$^{-/-}$ mice. We also labelled RBCs with 5-chloromethylfluorescein diacetate (CMFDA)[18]. We then measured the loss of CMFDA-labelled wild-type or *Nix*$^{-/-}$ RBCs after transfer into wild-type recipient mice. We observed accelerated clearance of transferred *Nix*$^{-/-}$ RBCs compared to wild-type controls (Fig. 2a, bottom panel). These data suggest that *Nix*$^{-/-}$ RBCs have a shorter lifespan *in vivo*.

Consistent with decreased survival of *Nix*$^{-/-}$ RBCs *in vivo*, spontaneous caspase activation was observed in *Nix*$^{-/-}$ but not wild-type RBCs after *in vitro* culture (Fig. 2b, c). Moreover, mitochondrion-containing RBCs from *Nix*$^{-/-}$ mice displayed phosphatidylserine, a signal for phagocytosis[19], before and after *in vitro* culture, as revealed by annexin V staining (Fig. 2d). A pan-caspase inhibitor, quinolyl-valyl-*O*-methylaspartyl-[2,6-difluorophenoxy]-methyl ketone (qVD-oph)[20], blocked caspase activation and suppressed annexin V staining on *Nix*$^{-/-}$ RBCs (Fig. 2c, e), indicating that caspase activation contributed to phosphatidylserine display. Increased ROS was detected in *Nix*$^{-/-}$ RBCs, and ROS scavengers inhibited caspase activation in *Nix*$^{-/-}$ RBCs (Fig. 2e). In agreement with accelerated clearance of RBCs, histochemistry showed increased iron-laden macrophages in the spleens of *Nix*$^{-/-}$ mice (Fig. 2f). Decreases in mature erythrocytes have been shown to induce compensatory erythropoiesis[13]. Consistently, reduced mature RBCs were correlated with increased erythropoietin mRNA and an expansion of Ter119^{+}CD71^{+} erythroblasts in *Nix*$^{-/-}$ mice (Fig. 2g and Supplementary Fig. 8). The increased erythropoietin may contribute to the expansion of Ter119^{+} CD71^{+} erythroblasts, thus ameliorating the anaemia in *Nix*$^{-/-}$ mice. Together, our data suggest that mitochondrial retention in *Nix*$^{-/-}$ RBCs results in increased caspase activation and phosphatidylserine display, leading to faster clearance of RBCs and compensatory

erythropoiesis. Removing mitochondria by autophagy would limit mitochondrial disruption in the cytosol and prevent the induction of apoptosis signalling in RBCs.

To induce the generation of sufficient numbers of reticulocytes for analyses, we treated mice with phenylhydrazine (PHZ), which induces reticulocytosis[21]. $Ter119^+$ $CD71^+$ reticulocytes in the peripheral blood were then sorted either on day 3 or on day 6 after PHZ treatment. Notably, a significant portion of the freshly sorted wild-type reticulocytes (18% at day 3 and 37% at day 6 after PHZ treatment) had already lost their mitochondria (Fig. 3a, top row). In contrast, fewer $Nix^{-/-}$ reticulocytes were negative for mitochondrial staining (Fig. 3a). This implies that $Nix^{-/-}$ reticulocytes were undergoing less efficient elimination of the mitochondria *in vivo*. After culture for *in vitro* maturation[3], $Nix^{-/-}$ reticulocytes showed significant delays in the removal of the mitochondria compared to wild-type controls (Fig. 3a and Supplementary Fig. 4a). This suggests that $Nix^{-/-}$ reticulocytes are defective in clearing mitochondria during maturation.

Inhibition of autophagy with 3-methyladenine, wortmannin or chloroquine[22,23] suppressed the removal of mitochondria but not ribosomes in reticulocytes (Supplementary Fig. 5), indicating that the clearance of mitochondria, but not ribosomes, is dependent on autophagy in RBCs. Abnormal autophagosome formation in $Nix^{-/-}$ reticulocytes might lead to defective mitochondrial clearance. We therefore stained reticulocytes for the processed form of microtubule-associated protein light chain 3 (LC3) that is characteristic of autophagosome formation[24]. Wild-type and $Nix^{-/-}$ reticulocytes had similar levels of LC3 punctate staining at the initiation of culture (Fig. 3c; LC3 dots per cell at day 0: wild type, 19.7 ± 3.9; $Nix^{-/-}$, 21.3 ± 4.5; $P=0.19$), indicating that the formation of autophagosomes was normal in the absence of Nix. Notably, LC3 co-localized with COX IV in wild-type but not $Nix^{-/-}$ reticulocytes (Fig. 3c). Moreover, wild-type but not $Nix^{-/-}$ reticulocytes had lost most COX IV staining by day 4 of *in vitro* culture (Fig. 3c). Electron microscopy showed that autophagic vacuoles in wild-type reticulocytes contained engulfed mitochondria; however, most mitochondria remained clustered outside of the autophagic vacuoles in $Nix^{-/-}$ reticulocytes (Fig. 3d and Supplementary Fig. 6). This suggests that Nix has a specific role in targeting the mitochondria into autophagosomes for clearance. In contrast to defective mitochondrial removal, $Nix^{-/-}$ RBCs showed no retention of the nucleus and underwent the loss of reticular staining similar to wild-type cells (Fig 1a, and Fig 3b and Supplementary Fig. 3c). Therefore, Nix seems to be required for the clearance of mitochondria, but not the nucleus or ribosomes, during erythroid maturation.

Incubation of Nix with purified mitochondria induced the loss of $\Delta\Psi_m$ (ref. 9). Wild-type reticulocytes showed continued decreases in $\Delta\Psi_m$ that preceded mitochondrial removal during *in vitro* maturation, whereas $Nix^{-/-}$ reticulocytes were defective in the loss of $\Delta\Psi_m$ (Supplementary Fig. 7a). This supports a role for Nix in disrupting $\Delta\Psi_m$ during erythroid maturation. Treatment with carbonyl cyanide *p*-trifluoromethoxyphenylhydrazone (FCCP), an uncoupling agent that dissipates the proton gradient across mitochondrial inner membrane to abolish $\Delta\Psi_m$ (ref. 25) (Supplementary Fig. 7c, d), promoted the clearance of mitochondria and restored the entry of the mitochondria into autophagic vacuoles in $Nix^{-/-}$ reticulocytes (Fig. 4a, b and Supplementary Fig. 4b). A BH3 mimetic, ABT-737 (ref. 26), which induced the loss of $\Delta\Psi_m$ (Supplementary Fig. 7c), also restored the entry of mitochondria into autophagosomes and promoted mitochondrial removal in $Nix^{-/-}$ reticulocytes (Fig. 4a, c and Supplementary Fig. 4b). ABT-737 has been shown to promote the initiation of autophagy by releasing beclin 1 from the suppression mediated by Bcl-2 or Bcl-xL[27]. Because Nix is not required for autophagosome formation (Fig. 3c), ABT-737 potentially rescued mitochondrial autophagy in $Nix^{-/-}$ reticulocytes by inducing the loss of $\Delta\Psi_m$. Although a BH3 mimetic can rescue the defects in $Nix^{-/-}$ RBCs, deletion of another BH3-only molecule, Bim, did not affect erythroid

differentiation (Supplementary Fig. 8). Therefore, Nix may be a specific sensor triggered by maturation signals in reticulocytes to promote mitochondrial autophagy.

Our study identifies an unexpected function for Nix in mitochondrial autophagy during erythroid differentiation. Nix-dependent loss of $\Delta\Psi_m$ may induce the display of molecules on the outer surface of mitochondria for recognition and sequestration by autophagosomes (Supplementary Fig. 1). Two yeast mitochondrial proteins, Uth1p (ref. 28) and Aup1p (ref. 29), have been shown to regulate mitochondrial autophagy in yeast. Here, we provide an example of specific regulation of mitochondrial autophagy in mammalian cells. Defective mitochondrial removal in *Nix*$^{-/-}$ RBCs was associated with spontaneous caspase activation, increased phosphatidylserine display and accelerated clearance by macrophages. Defective autophagy-dependent maturation and increased RBC clearance may contribute to anaemia in *Nix*$^{-/-}$ mice. In human K562 cells that were induced to undergo erythroid maturation, Nix-dependent removal of mitochondria was also observed (Supplementary Fig. 9). Defects in autophagic maturation of erythroid cells have been linked to anaemia in both humans and mice[4,14]. Understanding the mechanisms for mitochondrial autophagy in erythroid cells should facilitate the development of novel therapeutic approaches for treating haematological disorders involving defective erythroid maturation. It may also shed light on the mechanisms underlying mitochondrial quality control by autophagy in the protection against ageing, cancer and neurodegenerative diseases[30].

METHODS SUMMARY

Mice

A mouse embryonic stem cell clone with a gene trap insertion targeting the *Nix* locus (The Sanger Institute Gene Trap Consortium) was used to generate *Nix*$^{-/-}$ mice (Supplementary Fig. 2). Mice were backcrossed to the C57BL/6 background for more than five generations.

Analyses of autophagosomes

RBCs were incubated with mouse anti-COX IV (Invitrogen) and a rabbit antibody to processed LC3 (Abgent), followed with Alexa Fluro-conjugated secondary antibodies (Molecular Probes). The slides were examined by deconvolution microscopy (Applied Precision). RBCs were also fixed and embedded in Spurr's low-viscosity resin, and the sections were prepared and stained with uranyl acetate and lead citrate for analyses by transmission electron microscopy.

Analyses of apoptosis signalling

Cell lysates were used for SDS–PAGE and western blot analysis by probing with antibodies to different caspases, followed by incubation with horseradish peroxidase-conjugated secondary antibodies and developed by the chemiluminescent method (Pierce). Caspase activities were also measured using Ac-DEVD-pNA caspase-Glo reagent (Promega). To measure the display of phosphatidylserine on the cell surface, RBCs labelled with Mitotracker deep red were incubated with FITC–annexin V and analysed by flow cytometry.

Full Methodand any associated references are available in the online version of the paper at http://www.nature.com/nature.

METHODS

Mice

A mouse embryonic stem cell clone with a gene trap insertion targeting the *Nix* locus (The Sanger Institute Gene Trap Consortium) was used to generate $Nix^{-/-}$ mice (Supplementary Fig. 2). Mice were backcrossed to the C57BL/6 background for more than five generations.

Flow cytometry and immunocytochemistry

Erythroid cells from peripheral blood, bone marrow or spleen of wild-type and $Nix^{-/-}$ mice were stained with FITC–anti-CD71 and phycoerythrin–anti-Ter119 (BD Bioscience). Phosphatidylserine display was measured by staining with FITC–annexin V (BD Biosciences). To stain mitochondria, wild-type and $Nix^{-/-}$ RBCs were labelled with 200 nM Mitotracker deep red (Molecular Probes) at 37 °C for 30 min. The cells were then stained with FITC–anti-CD71 and phycoerythrin–anti-Ter119 and analysed by flow cytometry. For immunocytochemistry analyses, RBCs from wild-type and $Nix^{-/-}$ mice were stained with FITC–anti-CD71 and applied to slides by cytospin. The cells were fixed, incubated with mouse anti-COX IV (Invitrogen) and Alexa Fluor-conjugated secondary antibody. For mitochondria and LC3 co-staining, wild-type and $Nix^{-/-}$ RBCs were incubated with mouse anti-COX IV (Invitrogen) and a rabbit antibody to processed LC3 (Abgent), followed by staining with Alexa Fluor-conjugated secondary antibodies (Molecular Probes). The slides were examined using an AxioPlan2 fluorescent microscope (Zeiss) or a SoftWorx Image deconvolution microscope (Applied Precision). The Pearson coefficiency of correlation for LC3 and COX IV co-localization was determined by using the SoftWorx software (Applied Precision), with a value greater than 0.5 considered to have co-localization between the two signals.

Measurement of clearance of RBCs

Wild-type and $Nix^{-/-}$ mice were injected intravenously with (150 mg kg^{-1} body weight) NHS-biotin (Pierce), which covalently binds to free amino groups of cell surface proteins[17]. Cell clearance was determined by the loss of biotinylated RBCs[17]. RBCs were collected at indicated time points and the cells were incubated with phycoerythrin–Streptavidin (BD Bioscience). The percentage of labelled cells was analysed by flow cytometry. RBCs of wild-type or $Nix^{-/-}$ mice were also labelled with 4mM CMFDA (Molecular Probes) which emits green fluorescence after cleavage by intracellular esterases[18]. The labelled cells were injected into wild-type recipient mice intravenously. Blood was collected at indicated time points to quantify CMFDA-labelled cells by flow cytometry.

Induction of reticulocytosis in mice

Mice were injected intraperitoneally on day −1 and day 0 with phenylhydrazine (PHZ, Sigma; 60 mg kg^{-1} body weight). $Ter119^{+}CD71^{+}$ reticulocytes were then sorted on day 3 or day 6 after PHZ treatment using a FACSAria cell sorter (BD Bioscience).

Transmission electron microscopy

RBCs of wild-type and $Nix^{-/-}$ mice were fixed and embedded in Spurr's low viscosity resin similar to described protocols[31]. Sections were prepared and stained with uranyl acetate and lead citrate, followed by analyses using a Hitachi H-7500 transmission electron microscope.

Quantitative real-time RT–PCR

RNA was isolated from kidneys of 6-week-old wild-type and $Nix^{-/-}$ mice using the MELT total nucleic acid isolation system (Ambion). Erythropoietin mRNA was quantified by real-time RT–PCR and normalized against 18S RNA as described[32].

Analyses of apoptosis signalling

Cell lysates were used for SDS–PAGE and western blot analysis by probing with antibodies to Nix (Kamiya), caspase-6, caspase-9 (Cell Signaling), or actin (Santa Cruz Biotechnology), followed by incubation with horseradish peroxidase-conjugated secondary antibodies (Southern Biotechnology). The blots were developed by the chemiluminescent method (Pierce). To detect caspase activities, cells were added to 96-well plates with caspase-Glo reagent containing Ac-DEVD-pNA (Promega) and incubated at room temperature for 2 h. The relative luminescence unit (RLU) was measured in a luminometer (Labsystems). In some experiments, $Nix^{-/-}$ RBCs were cultured with solvent control, 4,000 U ml^{-1} catalase, 100 μM butylated hydroxytoluene, 5 μM tempol or 200 μM qVD-oph for 24 h. Caspase activities were measured as above. To measure the display of phosphatidylserine on the cell surface, RBCs with or without Mitotracker deep red labelling were incubated with FITC–annexin V (BD Biosciences) and analysed by flow cytometry. To measure ROS, wild-type and $Nix^{-/-}$ RBCs were cultured *in vitro* and stained with 20 μM 2′,7′-dichlorofluorescin diacetate. Mean fluorescent intensity (MFI) was plotted.

Statistical analysis

Data were presented as the mean ± s.e.m. and *P* values were determined by two-tailed Student's *t*-test using GraphPad Prism software version 4.0 for Macintosh.

Supplementary Material

Refer to Web version on PubMed Central for supplementary material.

Acknowledgements

We thank L. Huang, D. Yoon, A. Syed and D. Townley for technical assistance, and M. Andreeff for ABT-737. This work was supported by grants from the American Society of Hematology (M.C.), the American Heart Association (M.C.) and the NIH (J.W. and J.T.P.), a VA Merit grant (P.T.) and by a Ruth L. Kirschstein National Research Service Award (H.S.).

References

1. Yoshida H, et al. Phosphatidylserine-dependent engulfment by macrophages of nuclei from erythroid precursor cells. Nature 2005;437:754–758. [PubMed: 16193055]
2. Fader CM, Colombo MI. Multivesicular bodies and autophagy in erythrocyte maturation. Autophagy 2006;2:122–125. [PubMed: 16874060]
3. Koury MJ, Koury ST, Kopsombut P, Bondurant MC. *In vitro* maturation of nascent reticulocytes to erythrocytes. Blood 2005;105:2168–2174. [PubMed: 15528310]
4. Kent G, Minick OT, Volini FI, Orfei E. Autophagic vacuoles in human red cells. Am. J. Pathol 1966;48:831–857. [PubMed: 5937781]
5. Heynen MJ, Verwilghen RL. A quantitative ultrastructural study of normal rat erythroblasts and reticulocytes. Cell Tissue Res 1982;224:397–408. [PubMed: 7105141]
6. Takano-Ohmuro H, Mukaida M, Kominami E, Morioka K. Autophagy in embryonic erythroid cells: its role in maturation. Eur. J. Cell Biol 2000;79:759–764. [PubMed: 11089924]
7. Chen G, et al. Nix and Nip3 form a subfamily of pro-apoptotic mitochondrial proteins. J. Biol. Chem 1999;274:7–10. [PubMed: 9867803]
8. Imazu T, et al. Bcl-2/E1B 19 kDa-interacting protein 3-like protein (Bnip3L) interacts with bcl-2/Bcl-xL and induces apoptosis by altering mitochondrial membrane permeability. Oncogene 1999;18:4523–4529. [PubMed: 10467396]
9. Diwan A, et al. Unrestrained erythroblast development in $Nix^{-/-}$ mice reveals a mechanism for apoptotic modulation of erythropoiesis. Proc. Natl Acad. Sci. USA 2007;104:6794–6799. [PubMed: 17420462]

10. Aerbajinai W, Giattina M, Lee YT, Raffeld M, Miller JL. The proapoptotic factor Nix is coexpressed with Bcl-xL during terminal erythroid differentiation. Blood 2003;102:712–717. [PubMed: 12663450]
11. Kina T, et al. The monoclonal antibody TER-119 recognizes a molecule associated with glycophorin A and specifically marks the late stages of murine erythroid lineage. Br. J. Haematol 2000;109:280–287. [PubMed: 10848813]
12. Pan BT, Johnstone RM. Fate of the transferrin receptor during maturation of sheep reticulocytes *in vitro*: selective externalization of the receptor. Cell 1983;33:967–978. [PubMed: 6307529]
13. Socolovsky M, et al. Ineffective erythropoiesis in Stat5a$^{-/-}$5b$^{-/-}$ mice due to decreased survival of early erythroblasts. Blood 2001;98:3261–3273. [PubMed: 11719363]
14. Holm TM, et al. Failure of red blood cell maturation in mice with defects in the high-density lipoprotein receptor SR-BI. Blood 2002;99:1817–1824. [PubMed: 11861300]
15. Sivilotti ML. Oxidant stress and haemolysis of the human erythrocyte. Toxicol. Rev 2004;23:169–188. [PubMed: 15862084]
16. Raha S, Robinson BH. Mitochondria, oxygen free radicals, and apoptosis. Am. J. Med. Genet 2001;106:62–70. [PubMed: 11579426]
17. Hoffmann-Fezer G, et al. Biotin labeling as an alternative nonradioactive approach to determination of red cell survival. Ann. Hematol 1993;67:81–87. [PubMed: 8347734]
18. Levin J, et al. Pathophysiology of thrombocytopenia and anemia in mice lacking transcription factor NF-E2. Blood 1999;94:3037–3047. [PubMed: 10556187]
19. Fadok VA, Bratton DL, Frasch SC, Warner ML, Henson PM. The role of phosphatidylserine in recognition of apoptotic cells by phagocytes. Cell Death Differ 1998;5:551–562. [PubMed: 10200509]
20. Caserta TM, Smith AN, Gultice AD, Reedy MA, Brown TL. Q-VD-OPh, a broad spectrum caspase inhibitor with potent antiapoptotic properties. Apoptosis 2003;8:345–352. [PubMed: 12815277]
21. Vannucchi AM, et al. Accentuated response to phenylhydrazine and erythropoietin in mice genetically impaired for their GATA-1 expression (GATA-1^{low} mice). Blood 2001;97:3040–3050. [PubMed: 11342429]
22. Lum JJ, et al. Growth factor regulation of autophagy and cell survival in the absence of apoptosis. Cell 2005;120:237–248. [PubMed: 15680329]
23. Blommaart EF, Krause U, Schellens JP, Vreeling-Sindelarova H, Meijer AJ. The phosphatidylinositol 3-kinase inhibitors wortmannin and LY294002 inhibit autophagy in isolated rat hepatocytes. Eur. J. Biochem 1997;243:240–246. [PubMed: 9030745]
24. Kabeya Y, et al. LC3, GABARAP and GATE16 localize to autophagosomal membrane depending on form-II formation. J. Cell Sci 2004;117:2805–2812. [PubMed: 15169837]
25. Gottlieb E, Vander Heiden MG, Thompson CB. Bcl-x(L) prevents the initial decrease in mitochondrial membrane potential and subsequent reactive oxygen species production during tumor necrosis factor α-induced apoptosis. Mol. Cell. Biol 2000;20:5680–5689. [PubMed: 10891504]
26. Oltersdorf T, et al. An inhibitor of Bcl-2 family proteins induces regression of solid tumours. Nature 2005;435:677–681. [PubMed: 15902208]
27. Maiuri MC, et al. Functional and physical interaction between Bcl-X(L) and a BH3-like domain in Beclin-1. EMBO J 2007;26:2527–2539. [PubMed: 17446862]
28. Kissova I, Deffieu M, Manon S, Camougrand N. Uth1p is involved in the autophagic degradation of mitochondria. J. Biol. Chem 2004;279:39068–39074. [PubMed: 15247238]
29. Tal R, Winter G, Ecker N, Klionsky DJ, Abeliovich H. Aup1p, a yeast mitochondrial protein phosphatase homolog, is required for efficient stationary phase mitophagy and cell survival. J. Biol. Chem 2007;282:5617–5624. [PubMed: 17166847]
30. Tatsuta T, Langer T. Quality control of mitochondria: protection against neurodegeneration and ageing. EMBO J 2008;27:306–314. [PubMed: 18216873]
31. Koury ST, Koury MJ, Bondurant MC. Cytoskeletal distribution and function during the maturation and enucleation of mammalian erythroblasts. J. Cell Biol 1989;109:3005–3013. [PubMed: 2574178]

32. Mok H, Mendoza M, Prchal JT, Balogh P, Schumacher A. Dysregulation of ferroportin 1 interferes with spleen organogenesis in polycythaemia mice. Development 2004;131:4871–4881. [PubMed: 15342464]

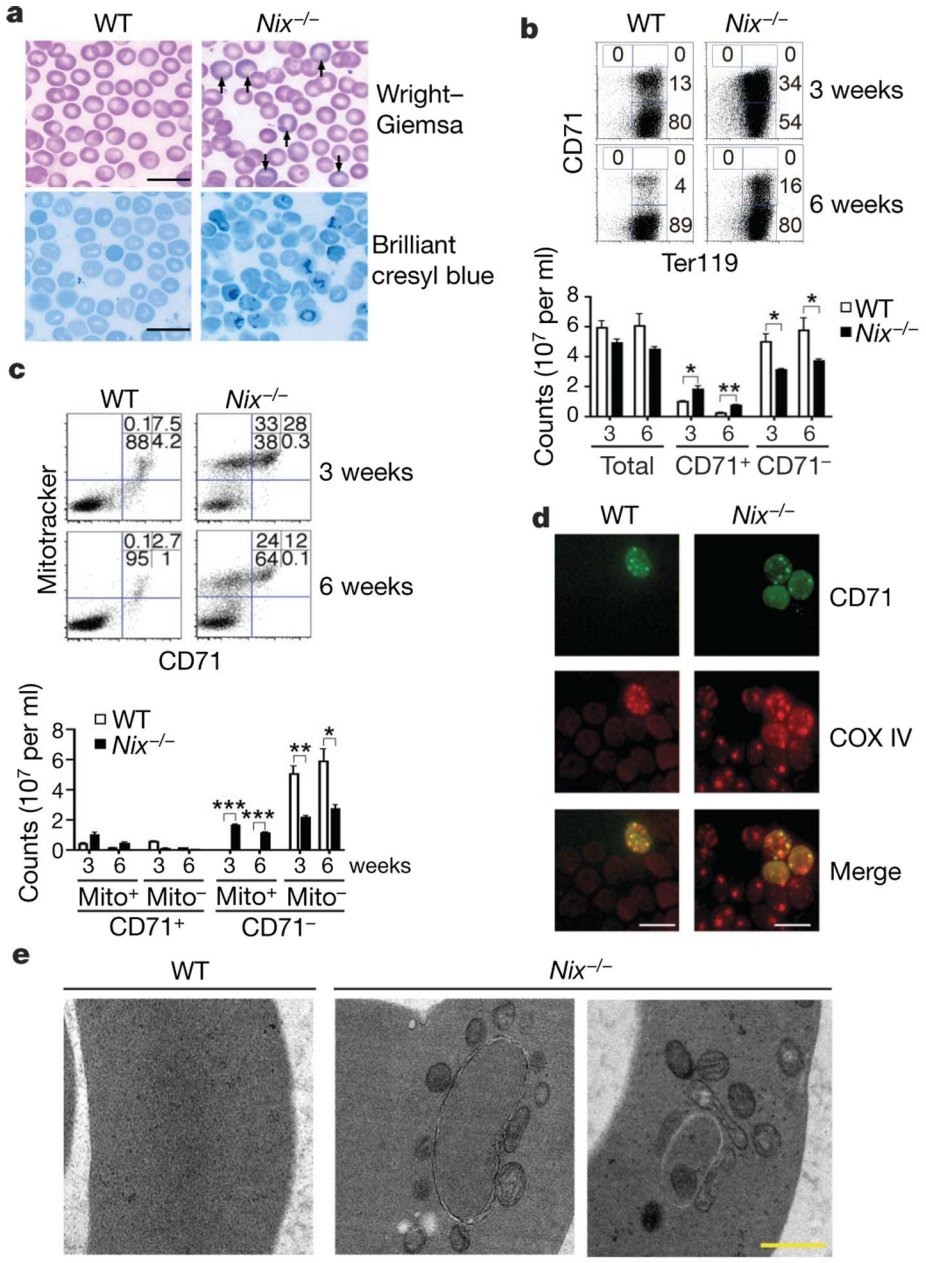

Figure 1. Reticulocytosis and retention of mitochondria in *Nix*$^{-/-}$ RBCs

a, Polychromasia (Wright–Giemsa stain, indicated by arrows) and increased reticulocytes (brilliant cresyl blue stain) revealed by staining blood smears from 6-week-old wild-type (WT) or *Nix*$^{-/-}$ mice (scale bar, 20 μm). **b**, **c**, Ter119 (**b**) or Mitotracker deep red (**c**) versus CD71 staining of RBCs from 3- or 6-week-old mice. Cell counts were also calculated (mean ± s.e.m.; $n = 3$). *P <0.05; **P <0.01; ***P<0.001. **d**, **e**, Analyses of RBCs as in **b** by immunocytochemistry (**d**; scale bar, 10 μm) or transmission electron microscopy (**e**; scale bar, 0.5 μm).

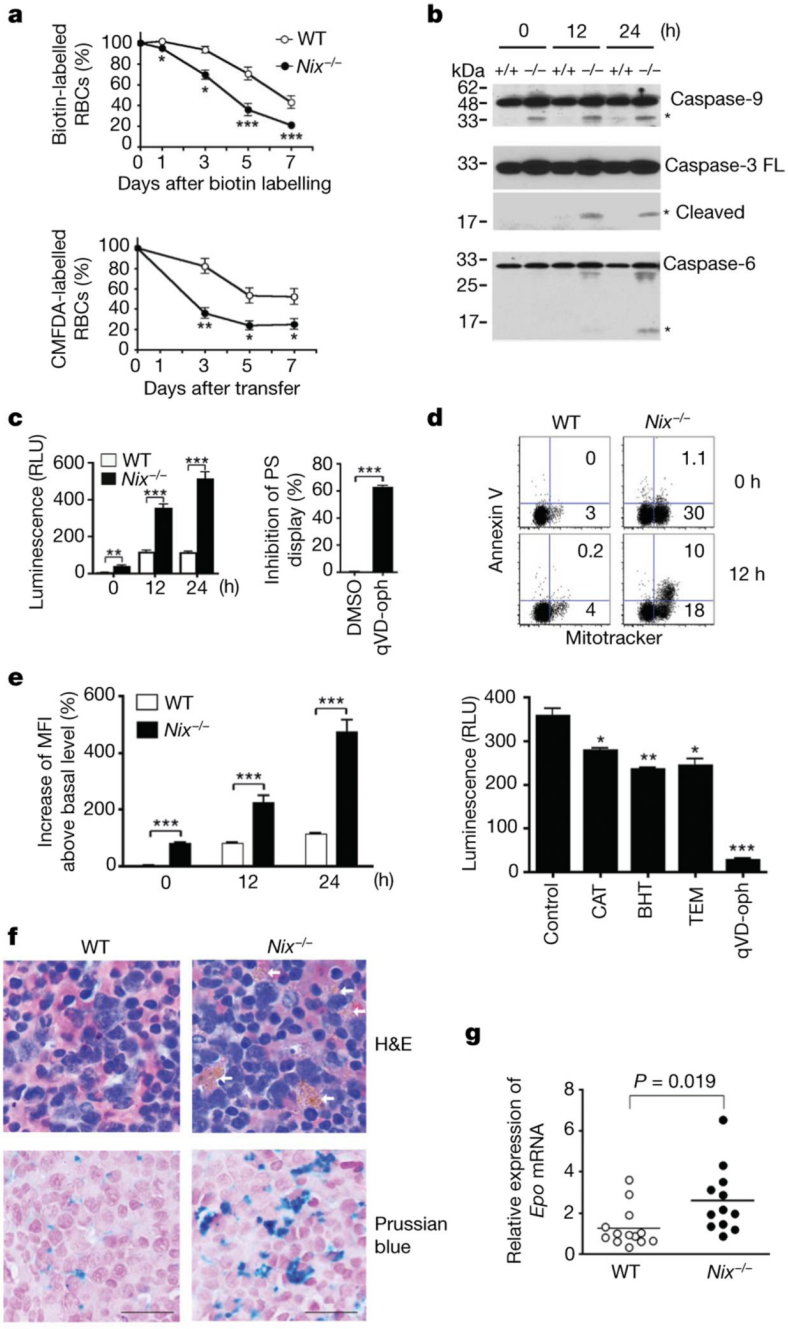

Figure 2. Decreased survival of RBCs in *Nix*$^{-/-}$ mice

a, Quantification of NHS-biotin-labelled RBCs or transferred CMFDA-labelled RBCs ($n = 3$). **b**, Western blot analyses of caspases in RBCs after *in vitro* culture. Asterisks denote processed caspases. FL, full length. **c**, The relative luminescence units (RLU) of caspase activities in cultured RBCs and the suppression of annexin V staining in *Nix*$^{-/-}$ RBCs after 12-h culture in the presence of qVD-oph or solvent control (DMSO) ($n = 3$). **d**, Mitotracker versus annexin V staining of RBCs after *in vitro* culture. **e**, Mean fluorescent intensity (MFI) of ROS staining in RBCs after *in vitro* culture, and caspase activities in *Nix*$^{-/-}$ RBCs after 24 h culture with solvent control, ROS scavengers or qVD-oph ($n = 3$). BHT, butylated hydroxytoluene; CAT, catalase; TEM, tempol.

f, Haematoxylin and eosin (H&E) staining of spleen sections of 9-week-old wild-type and *Nix*$^{-/-}$ mice. Arrows denote iron deposits within macrophage cytoplasm. Iron deposits were also stained with Prussian blue, followed by counterstain with nuclear-fast red. Scale bar, 20 μm. **g**, Real-time RT–PCR of erythropoietin (*Epo*) (n = 12). For all relevant panels, statistical significance of the data (mean ± s.e.m.) is: *P<0.05; **P<0.01; ***P<0.001.

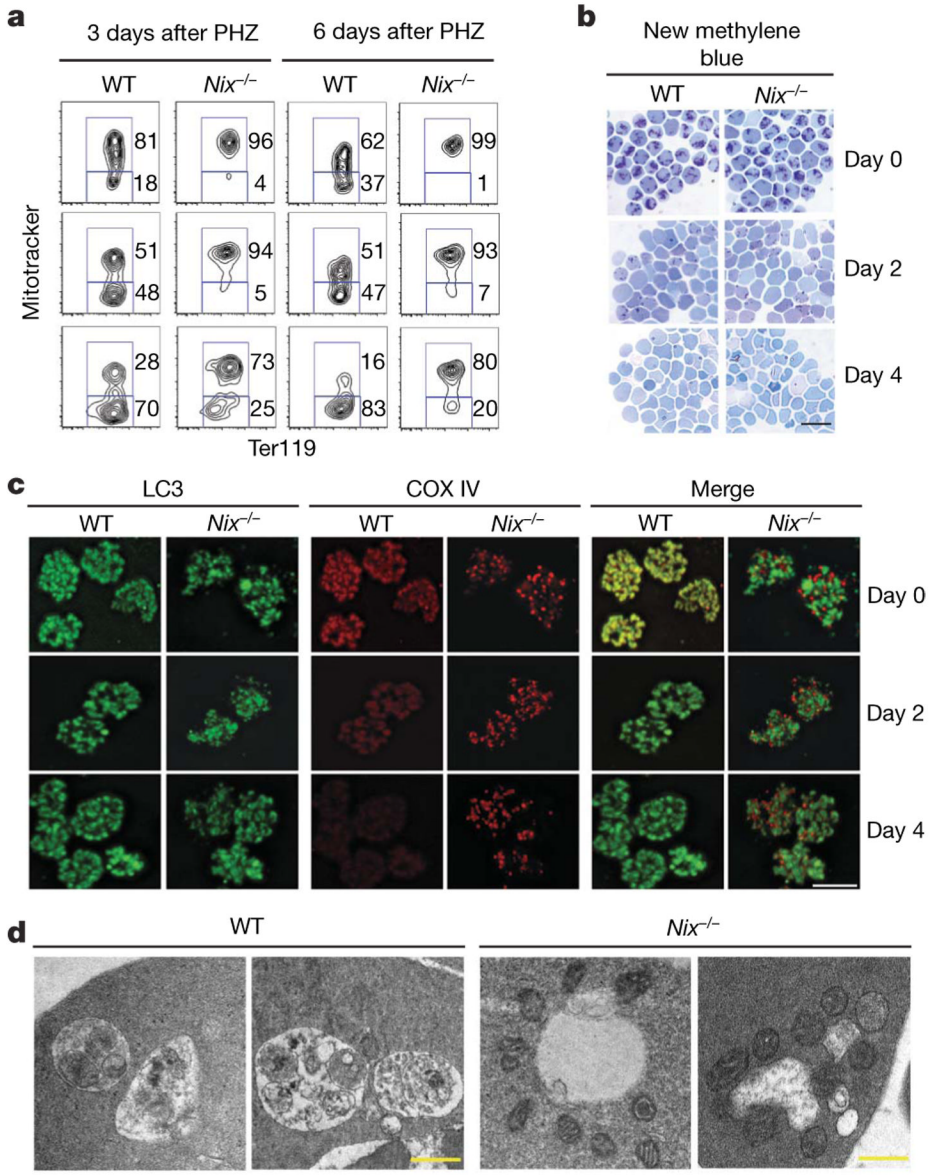

Figure 3. Defective clearance of mitochondria by autophagy in *Nix*$^{-/-}$ reticulocytes

a, Ter119^{+} CD71^{+} reticulocytes sorted at day 3 or 6 after PHZ treatment were cultured for *in vitro* maturation for 0 (top row), 2 (middle row) or 4 (bottom row) days, followed by Mitotracker deep red and Ter119 staining. **b**, CD71^{+} Ter119^{+} reticulocytes sorted at day 3 after PHZ treatment were cultured and stained with new methylene blue. Scale bar, 20 μm. **c**, Cells as in **b** were stained for LC3 and COX IV and analysed by deconvolution microscopy. Scale bar, 5 μm. The Pearson coefficiency for LC3 and COX IV co-localization at day 0 (mean ± s.e.m.) is: wild type, 0.81 ± 0.001; *Nix*$^{-/-}$, 0.44 ± 0.036 (n = 35, P = 0.0006). **d**, Cells sorted as in **b** were analysed by electron microscopy. Scale bar, 0.5 μm.

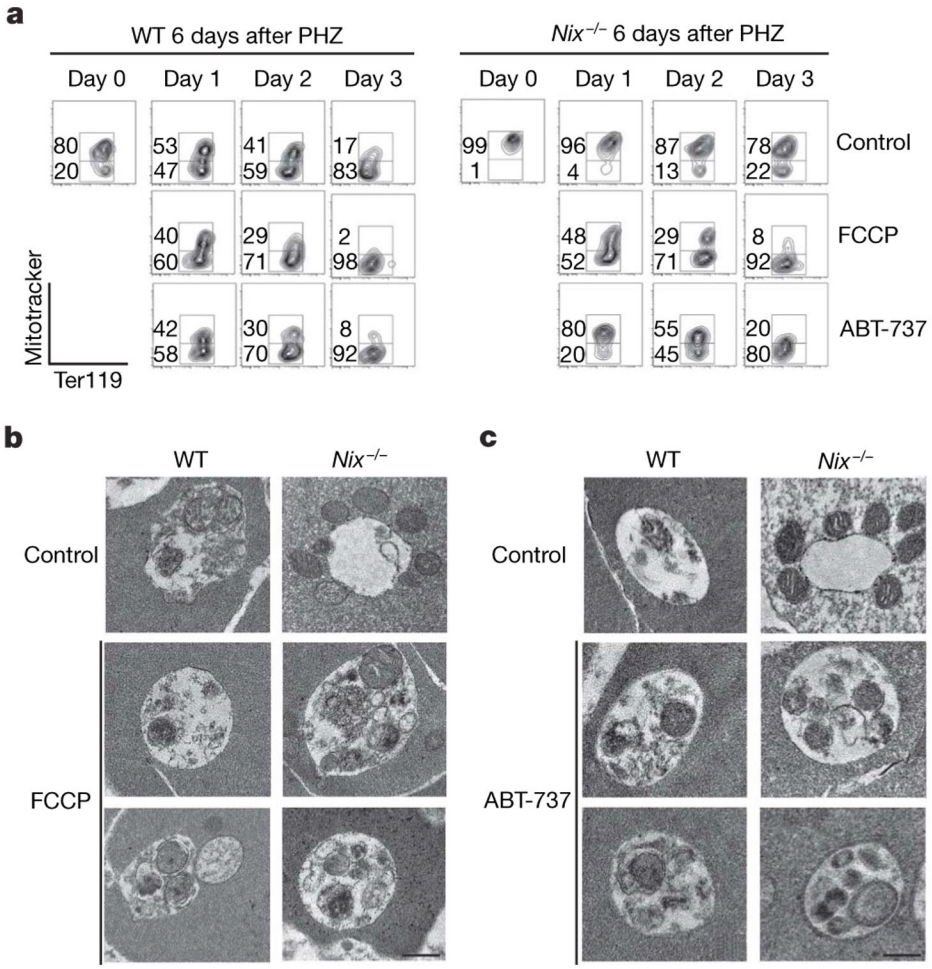

Figure 4. Removal of mitochondria by autophagy in FCCP-treated or ABT-737-treated *Nix*$^{-/-}$ reticulocytes

a, Ter119^{+} CD71^{+} reticulocytes were sorted from the peripheral blood of wild-type and *Nix*$^{-/-}$ mice at day 6 after PHZ treatment. The cells were cultured for *in vitro* maturation in the presence of 10 μM FCCP or 1 μM ABT-737, followed by staining with Mitotracker deep red and phycoerythrin-conjugated anti-Ter119. **b**, **c**, Reticulocytes were cultured with FCCP (**b**) or ABT-737 (**c**) for 24 h and analysed by transmission electron microscopy. Scale bar, 0.5 μm.